Bucknell University

Bucknell Digital Commons

Faculty Journal Articles

Faculty Scholarship

2011

Hydraulic Conductivity of Model Soil-Bentonite Backfills Subjected to Wet-Dry Cycling

Michael A. Malusis
Bucknell University, mam028@bucknell.edu

Jeffrey C. Evans
Bucknell University

SeungChoel Yeom
Drexel University

Follow this and additional works at: https://digitalcommons.bucknell.edu/fac_journ

Part of the Environmental Engineering Commons, and the Geotechnical Engineering Commons

Recommended Citation

Hydraulic conductivity of model soil–bentonite backfills subjected to wet–dry cycling

Michael A. Malusis, Seungcheol Yeom, and Jeffrey C. Evans

Abstract: The potential for changes in hydraulic conductivity, k, of two model soil–bentonite (SB) backfills subjected to wet–dry cycling was investigated. The backfills were prepared with the same base soil (clean, fine sand) but different bentonite contents (2.7 and 5.6 dry wt.%). Saturation (S), volume change, and k of consolidated backfill specimens (effective stress, 24 kPa) were evaluated over 3–7 cycles in which the matric suction, Ψ_m, in the drying stage ranged from 50 to 700 kPa. Both backfills exhibited susceptibility to degradation in k caused by wet–dry cycling. Mean values of k for specimens dried at $\Psi_m = 50$ kPa ($S = 30\%$–60% after drying) remained low after two cycles, but increased by 5–300-fold after three or more cycles. Specimens dried at $\Psi_m \geq 150$ kPa ($S < 30\%$ after drying) were less resilient and exhibited 500- to 10 000-fold increases in k after three or more cycles. The greater increases in k for these specimens correlated with greater vertical shrinkage upon drying. The findings suggest that increases in hydraulic conductivity due to wet–dry cycling may be a concern for SB vertical barriers located within the zone of a fluctuating groundwater table.

Key words: cutoff walls, desiccation, hydraulic conductivity, soil–bentonite, vertical barriers, wet–dry cycles.

Résumé : Cette étude vise à évaluer le potentiel de variation de la conductivité hydraulique, k, de deux modèles de remblais faits de sol et bentonite (SB) soumis à des cycles de mouillage–séchage. Les remblais ont été préparés avec le même sol de base (sable fin et propre) et avec des teneurs en bentonite différentes (2,7 et 5,6 % massique sec). La saturation (S), les variations de volume et k ont été évaluées sur des échantillons de remblai consolidé (contrainte effective, 24 kPa), et ce, pour 3–7 cycles, avec une succion matricielle, Ψ_m, variant de 50–700 kPa durant la période de séchage. Les valeurs moyennes de k pour les échantillons séchés à $\Psi_m = 50$ kPa ($S = 30$–60 % après séchage) sont demeurées basses après deux cycles, mais ont augmenté de 5–300 fois après trois cycles et plus. Les échantillons séchés à $\Psi_m \geq 150$ kPa ($S < 30$ % après séchage) étaient moins résilients et ont démontré des augmentations de k de 500 à 10 000 fois après trois cycles et plus. Les plus grandes augmentations de k pour ces échantillons correspondent à un retrait vertical plus important durant le séchage. Ces résultats suggèrent que les augmentations de la conductivité hydraulique causées par les cycles de mouillage–séchage peuvent être problématiques dans le cas de barrières verticales faites de SB situées à l'intérieur de la zone de fluctuations de la nappe phréatique.

Mots-clés : parafouille, dessiccation, conductivité hydraulique, sol–bentonite, barrière verticale, cycles de mouillage–séchage.

[Traduit par la Rédaction]

Introduction

Vertical barriers (i.e., cutoff walls) have been employed widely since the 1970's for groundwater control and in situ containment of subsurface pollutants. In the United States, the most common type of vertical barrier is the *soil–bentonite (SB) slurry trench cutoff wall*, which is named after the method of construction (slurry trench) and the nature of the barrier material (SB) (see LaGrega et al. 2001). The typical construction process for an SB vertical barrier involves ex-

cavating a trench while simultaneously filling the trench with bentonite–water slurry to maintain trench stability. The trench then is refilled with a high-slump SB backfill (i.e., typically trench spoils mixed with slurry and additional dry bentonite, if needed) that exhibits a low hydraulic conductivity, k (i.e., $10^{-10} \leq k \leq 10^{-8}$ m/s), necessary to impede groundwater flow and advective contaminant transport (Xanthakos 1979; D'Appolonia 1980; Evans 1993).

Potential uses of SB vertical barriers include applications in which effective hydraulic performance may be required over extended periods (e.g., decades). For example, SB barriers may be constructed within impoundment dikes or levees as a long-term solution for mitigating excessive seepage and potential instability (Owaidat et al. 1999; Andromalos and Fisher 2001). In addition, SB barriers often are used as an interim remedial strategy to minimize the spread of groundwater pollutants for an undefined period of time until a more efficient and (or) cost effective treatment technology is developed or until the pollutants are attenuated naturally (Shackelford and Jefferis 2000; Sharma and Reddy 2004). In such applications, the ability of the SB backfill to maintain a low

M.A. Malusis and J.C. Evans. Department of Civil and Environmental Engineering, Bucknell University, Lewisburg, PA 17837, USA.
S. Yeom. Department of Civil and Environmental Engineering, Bucknell University, Lewisburg, PA 17837, USA; Department of Civil, Architectural, and Environmental Engineering, Drexel University, Philadelphia, PA 19104, USA.

Corresponding author: M.A. Malusis (e-mail: michael.malusis@bucknell.edu).

k over time is paramount to the successful performance of the barrier. However, changes in k of SB backfill may occur long after construction due to factors such as cyclic wetting–drying and freezing–thawing, changes in stress, deformation cracking, and interaction between the bentonite and chemical constituents in the pore water (Evans 1993, 1995; Filz et al. 2003). These factors have been studied extensively for compacted liners and geosynthetic clay liners (GCLs) (e.g., Othman and Benson 1993; Boardman and Daniel 1996; Hewitt and Daniel 1997; Kraus et al. 1997; Petrov and Rowe 1997; Petrov et al. 1997; Stern and Shackelford 1998; Abichou et al. 2000; Lin and Benson 2000; Shackelford et al. 2000; Albrecht and Benson 2001; Kolstad et al. 2004*a*, 2004*b*; Jo et al. 2005, 2006; Southen and Rowe 2005; Podgorney and Bennett 2006; Benson and Meer 2009; Scalia and Benson 2010), but have received less attention for vertical barriers.

In particular, the potential for changes in k of SB backfill due to wet–dry cycling has been recognized as a medium- to long-term performance concern for vertical barriers (National Research Council 2007). In many SB barrier installations, the water levels on the inboard and (or) outboard sides of the barrier may fluctuate over time due to natural and (or) anthropogenic causes. As a result, some portion of an SB barrier may be located within the zone of a fluctuating water table and may dry when the water table is depressed. If this portion of the barrier does not maintain a low k upon rewetting when the water table rises, the overall effectiveness of the barrier may be compromised.

For example, consider a scenario in which an SB barrier is installed in a dike surrounding a surface impoundment, as illustrated schematically in Fig. 1. The permanently submerged portion of the barrier represents the portion below the phreatic surface corresponding to the lowest water level maintained in the impoundment (phreatic surface a). Whereas the permanently submerged backfill is expected to maintain a low k over time (unless detrimentally affected by contaminants in the water), the remainder of the barrier (above phreatic surface a) may be impacted by cyclic periods of potential desiccation as the impoundment water level rises and falls. Under the high water condition in Fig. 1, a properly functioning (low k) barrier will limit seepage through the dike (phreatic surface b). Conversely, a poorly functioning (high k) barrier that has been damaged by desiccation would allow greater seepage of water and any associated contaminants through the dike (phreatic surface c). This latter scenario also could lead to dike instability and failure.

Limited field evidence suggests that k of SB backfill may be affected by wet–dry cycling. For example, Evans (1994) conducted flexible-wall k tests (with tap water) on SB backfill specimens prepared from thin-walled tube samples recovered from two sections (i.e., a 4 year old section and a 10 year old section) of an in-service SB cutoff wall with a shallow adjacent groundwater table (~2 m below the ground surface). The measured k of backfill collected 1 m above the adjacent water table was ~50–100 000 times greater than the k of backfill collected 1 m below the adjacent water table, with the greatest disparity in k observed for the older of the two wall sections. The tests were repeated after several days of backpressure saturation, with no change in the results. Moreover, water content profiles within the wall sections re-

Fig. 1. Schematic illustration of flow through an SB vertical barrier installed in a dike. Phreatic surfaces a–c depict the following scenarios: a, low water conditions; b, flow through properly functioning (low k) wall under high water conditions; c, flow through damaged (high k) wall under high water conditions.
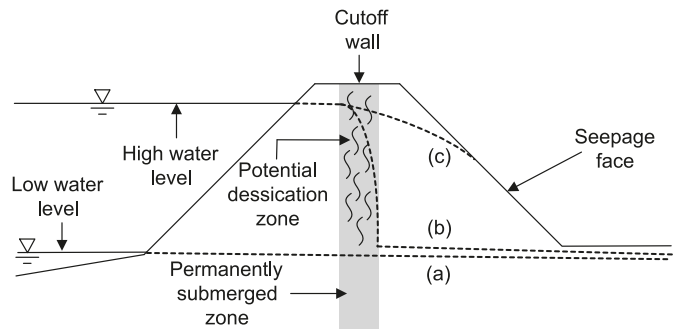
vealed that the water content had diminished within the portions of the wall sections that were 1 m above the adjacent water table, suggesting that the air-entry suction within the backfill was limited to <1 m in this case.

Based on the above considerations, the objective of this study is to investigate the potentially deleterious effect of wet–dry cycling on the hydraulic conductivity of SB backfill. The hydraulic and volume-change response of two model SB backfills subjected to wet–dry cycles are evaluated under controlled laboratory conditions. Relevant variables considered in the laboratory testing program include the number of cycles, the extent of drying in each cycle, and the bentonite content in the backfill. Measured moisture retention curves for the two model backfills also are presented for interpretive purposes, and recommendations for future work based on the findings and limitations of this study are provided.

Materials and methods

Solid materials

The model SB backfills tested in this study were prepared using clean sand, powdered sodium bentonite, and bentonite–water slurry. The sand is a fine, poorly graded sand excavated locally and provided by Central Builders Supply (Lewisburg, Pa.). This sand was chosen to represent a case of SB vertical barrier construction in which the hydraulic conductivity of the backfill is governed by the bentonite content and is not influenced significantly by the presence of native fines. The bentonite used in the study is a slurry-grade sodium bentonite that is commercially available under the trade name Naturalgel (Wyo-Ben, Inc., Billings, Mont.) and is marketed for SB barrier applications. Measured grain-size distributions (ASTM 2007) for the sand and bentonite are shown in Fig. 2. The sand is classified as poorly graded sand (SP) based on the Unified Soil Classification System (ASTM 2010*a*). The bentonite is classified as high-plasticity clay (CH) based on a measured liquid limit and plasticity index of 488 and 443, respectively (ASTM 2010*b*).

Backfill mixtures and specimen preparation

Bentonite–water slurry (5% bentonite by mass) was prepared by blending the bentonite with tap water (pH = 6.6; electrical conductivity, EC = 22.2 mS/m) in a Hamilton Beach (Washington, N.C.) seven-speed blender at the highest

Fig. 2. Grain-size distributions of sand and bentonite used to prepare model SB backfills.
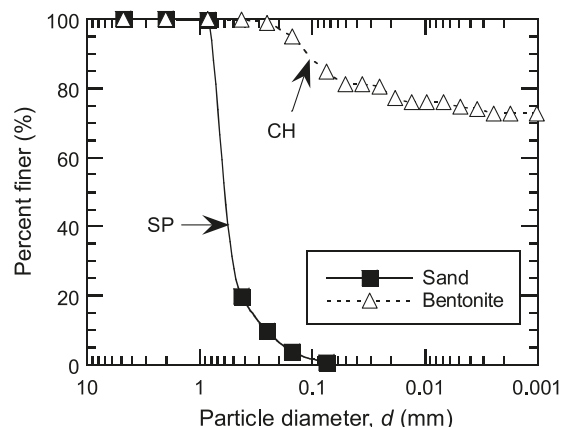
operating speed, simulating a colloidal shear mixer used in the field. The slurry was allowed to hydrate for a minimum of 24 h prior to use. After hydration, the measured density and Marsh cone viscosity of the slurry were 1.04 g/cm^3 and 38 s, respectively. Two model backfills were then prepared by combining the sand, slurry, and two different percentages of dry bentonite in a Hobart Corporation (Troy, Ohio) model N50 mixer to ensure uniformity. Slurry was added incrementally until the backfills exhibited a slump of 30–45 mm in a miniature slump cone with a height of 150 mm and top and bottom radii of 75 and 100 mm, respectively. This miniature cone slump range correlates to a standard cone (ASTM 2010c) slump range of 125 ± 25 mm (see Malusis et al. 2008), the range typically specified for SB vertical barriers (Evans 1993).

Mixture proportions for the model backfills (i.e., backfills B1 and B2) are summarized in Table 1. Different percentages of dry bentonite were added to backfills B1 and B2 (i.e., 1.3% and 3.9%, respectively) to evaluate the influence of bentonite content on the hydraulic and volume-change responses during wet–dry cycles. Also, backfill B2 required a greater mass of slurry than backfill B1 to achieve the aforementioned slump range. As a result, the gravimetric water content, w, and bentonite content from slurry were higher for backfill B2 relative to backfill B1. After addition of slurry, the total bentonite content in mixture B2 (5.6%) was approximately twice that in mixture B1 (2.7%). The narrow range of measured w for each backfill in Table 1 reflects only slight variability in measured w that occurred each time a new bulk volume of backfill was prepared, demonstrating that the backfill preparation process was effective for creating uniform backfills in a reproducible manner.

Test specimens were prepared by consolidating the backfill mixtures in GeoTest model S2800 fixed-ring consolidometers (GeoTest Instrument Corp., Evanston, Ill.). The backfills were placed into steel retaining rings (diameter, 63.5 mm; height, 25.4 mm) and rodded to eliminate large voids before excess material was struck from the top of each ring. The specimens were consolidated under an effective stress, σ', of 24 kPa for a minimum of 24 h. This value of σ' was chosen to simulate a low-stress condition expected at shallow depth within an SB vertical barrier, i.e., where wet–dry cycling of the backfill is most likely to occur. For example, $\sigma' =$

24 kPa is expected to correspond to a depth of <5 m within an SB vertical barrier based on a recent study by Ruffing et al. (2010). Upon completion of the consolidation stage, the baseline (initial) k to tap water was measured for each specimen using an upward-flow, falling head procedure (see Yeo et al. 2005; Malusis et al. 2009). Hydraulic gradients were maintained below 50 in all tests, and the specimens were permeated until (i) the measured k was within ±25% of the mean of the previous four consecutive measurements and (ii) no distinct upward or downward trend in k was observed (see Yeom 2010). Once the baseline k was obtained, the steel rings containing the specimens were removed from the consolidometers, and the dimensions and weight of each specimen (with ring) were measured before the specimens were subjected to drying.

Cyclic wet–dry tests

The consolidated backfill specimens were subjected to cyclic drying in leak-free pressure plate extractors (LFPPEs), as described by Wang and Benson (2004) and shown schematically in Fig. 3. The LFPPE apparatus consists of a brass cell in which the specimen (housed within the retaining ring) is placed on a saturated, porous ceramic disk (Soilmoisture Equipment Corp., Santa Barbara, Calif.), with an air-entry pressure of 1500 kPa. The ceramic disk is surrounded by a Buna-N square gasket to prevent leakage of air around the disk. The pore-water pressure in the specimen was maintained at zero (atmospheric pressure), while the air pressure inside the cell was elevated using compressed air (via the top port) to establish a prescribed value of matric suction (Ψ_m) by axis translation (see Fredlund and Rahardjo 1993). The water expelled from the specimen under the applied Ψ_m was monitored by tracking the migration of the air–water interface in a horizontal tube connected to the bottom drain port (see Fig. 3). Drying cycles were terminated after water expulsion in response to the applied Ψ_m was observed to be complete (i.e., the air–water interface became stationary). After drying, the weights and dimensions of the specimens were measured, and the specimens were returned to the consolidometers. The specimens were resubmerged and reloaded to $\sigma' = 24$ kPa for a minimum of 24 h prior to remeasurement of k (with tap water) using the same falling head procedure described previously.

Triplicate specimens of backfill B1 were subjected to drying cycles with applied $\Psi_m = 50$, 150, and 400 kPa, and triplicate specimens of backfill B2 were subjected to drying cycles with applied $\Psi_m = 50$, 400, and 700 kPa. Although the original intent was to test both backfills at $\Psi_m = 50$, 400, and 700 kPa, drying at $\Psi_m = 400$ kPa was sufficient to cause degradation in k of backfill B1 after only one drying cycle (see Results and discussion). Therefore, $\Psi_m = 150$ kPa was used in lieu of $\Psi_m = 700$ kPa for backfill B1. In addition, two specimens of backfill B1 and three specimens of backfill B2 were used as control (undried) specimens ($\Psi_m = 0$). These specimens were not placed in LFPPEs but otherwise were subjected to the same cyclic handling procedure (i.e., unloading, removal from the consolidometers, measurement of specimen weight and dimensions, reloading in the consolidometers, and remeasurement of k) as the dried specimens to determine the extent of any changes in k caused by the handling procedure. The number of cycles applied to a

Table 1. Compositions of model SB backfills tested in study.

Backfill	Bentonite content (dry wt.%)			Sand content (dry wt.%)	Gravimetric water content, w (%)
	From slurry	Additional (dry)	Total		
B1	1.4	1.3	2.7	97.3	33.9–35.4
B2	1.7	3.9	5.6	94.4	40.9–41.4

Fig. 3. Schematic of LFPPE apparatus (redrawn after Wang and Benson 2004).
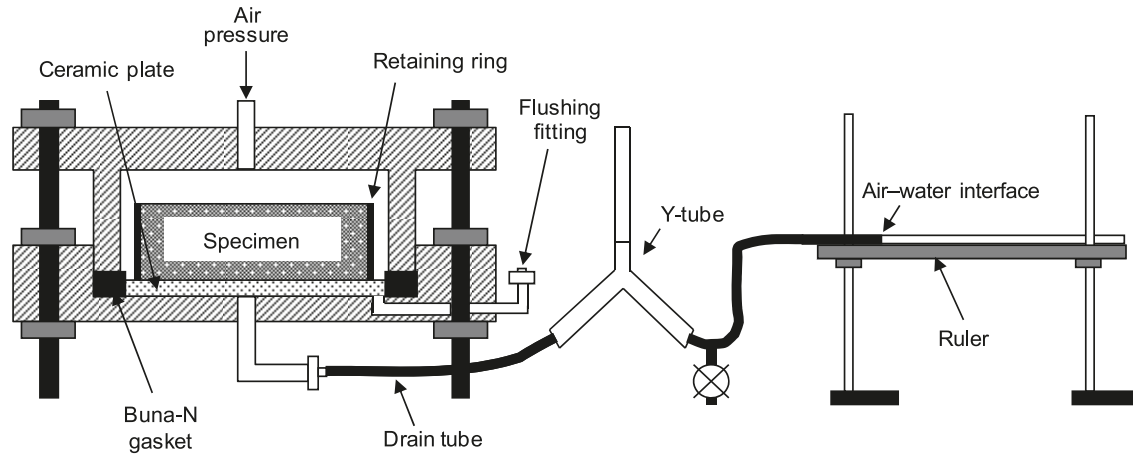
given set of replicate specimens ranged between three and seven cycles, depending upon the nature of the hydraulic responses of the individual specimens.

Soil-water retention curves

Soil-water retention curves (SWRCs; drying curves) were measured for each model backfill using a combination of pressure plate extraction and chilled-mirror hygrometry (ASTM 2008). The SWRCs were developed in parallel with the cyclic wet–dry tests and were used to evaluate whether or not the extent of drying in the cyclic tests was consistent with the water retention characteristics of the backfills. For the pressure plate portions of the SWRCs, one specimen of each backfill (prepared in the same manner as described above) was subjected to stepwise drying in an LFPPE. The applied Ψ_m in these tests ranged from 20 to 100 kPa for backfill B1 and from 20 to 570 kPa for backfill B2. The pressure plate test on backfill B1 was terminated at a lower value of applied Ψ_m due to excessive migration of air into the drain tube that confounded accurate measurement of expelled water volume.

A chilled mirror hygrometer (model WP4 dewpoint potentiameter, Decagon Devices, Inc., Pullman, Wash.) was used to develop the portions of the SWRCs for values of Ψ_m ranging from 200 to 100 000 kPa, i.e., above those applied in the LFPPEs. The hygrometer specimens were prepared by placing backfill into disposable sample cups (38 mm in diameter and 10 mm tall) such that each cup was half full and the dry unit weights were approximately the same as for the pressure plate specimens. The specimens were dried to known water contents and placed into the hygrometer, which measures the temperature of the specimen and the temperature at which condensation appears on a precisely chilled mirror located above the cup. These temperatures establish the vapor pressure of the overlying headspace and the corresponding water

potential (suction). Although the hygrometer yields values of total suction, Ψ_t, which represent the sum of Ψ_m and osmotic suction, Ψ_o (i.e., $\Psi_t = \Psi_m + \Psi_o$), the contribution of Ψ_o in dry soils is generally small such that $\Psi_t \approx \Psi_m$ (Fredlund and Rahardjo 1993; Wang and Benson 2004). Therefore, the pressure plate and hygrometer data were combined to form a single SWRC for each specimen. The SWRCs were fitted with the van Genuchten equation, which may be expressed as follows for an initially saturated porous medium (van Genuchten 1980):

$$[1] \quad \frac{S - S_r}{1 - S_r} = \left[\frac{1}{1 + (\alpha \Psi_m)^n} \right]^{1 - 1/n}$$

where S is saturation, S_r is residual saturation (i.e., the asymptotic value of S at high Ψ_m), and α and n are empirical fitting parameters that describe the shape of the SWRC.

Results and discussion

SWRCs

The SWRCs for the two model backfills are illustrated in Fig. 4. The smooth transition between the pressure plate and hygrometer portions of the SWRCs indicates that the two independent data sets for each backfill reflect similar water retention characteristics. Best-fit values of the van Genuchten parameters (α, n, and S_r), tabulated in Fig. 4, were obtained by nonlinear, least-squares regression of eq. [1]. Coefficients of determination (R^2) exceeded 0.95, indicating that the van Genuchten model was reasonable for describing the water retention behavior of the backfills.

Backfills B1 and B2 exhibit comparable water retention characteristics, despite the difference in bentonite content between the two backfills. Backfill B2 exhibits a slightly lower α and slightly higher n and S_r relative to backfill B1. These

Fig. 4. SWRCs, with corresponding van Genuchten regressions, for backfills B1 (2.7% bentonite) and B2 (5.6% bentonite). Tabulated values represent best-fit parameters (standard percent errors in parentheses).

Parameter	B1	B2
α (kPa^{-1})	0.0493 (16.7)	0.0381 (9.35)
n	1.78 (8.43)	1.94 (5.28)
S_r	0.0409 (84.6)	0.0829 (14.4)
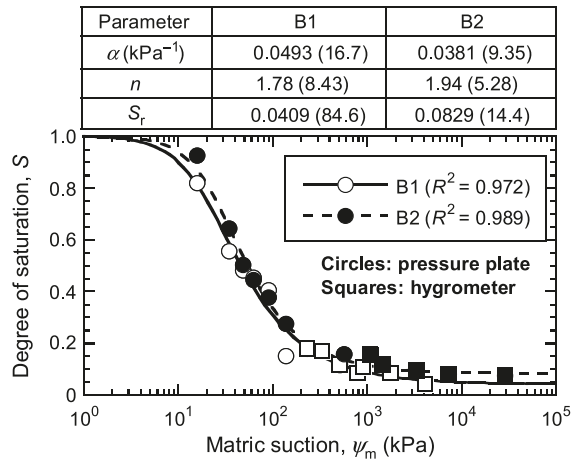
findings are consistent with the higher bentonite content in backfill B2. However, when the standard errors associated with the fitting parameters (see Fig. 4) are taken into account, differences in the SWRCs for the two backfills are not statistically significant at the 5% level (i.e., $p > 0.05$ from unpaired t test).

The air-entry suctions, Ψ_a, for the two backfills are in the range of 8–12 kPa based on extrapolation of the semi-log-linear portions of the SWRCs to $S = 1.0$ in Fig. 4 (see Fredlund and Rahardjo 1993; Tinjum et al. 1997). Thus, significant loss of saturation in the backfills was expected for the cyclic wet–dry tests in which $\Psi_m \geq 50$ kPa was employed. For example, the results in Fig. 4 indicate that application of a drying cycle with $\Psi_m = 50$ kPa would reduce S to ~50%, and $\Psi_m \geq 150$ kPa would reduce S to <30%.

Cyclic wet–dry tests

Saturation and volume change

The measured phase properties and k of all replicate backfill specimens subjected to wet–dry cycles are summarized in Tables 2 and 3 for backfills B1 and B2, respectively. Initial values (i.e., cycle 0) of specimen thickness (H), volume (V), S, void ratio (e), and k after consolidation ($\sigma' = 24$ kPa) were consistent for each replicate set of backfill specimens prepared at a given time using the same bulk mixture, again demonstrating the reproducibility of the specimen preparation procedures. Initial k values ranged from 5.3×10^{-8} to 1.7×10^{-7} cm/s for backfill B1 and from 1.9×10^{-8} to 2.4×10^{-8} cm/s for backfill B2, reflecting the difference in bentonite content between the two backfills. Also, all specimens were at or near complete saturation ($S > 93\%$) prior to the first drying cycle, as expected. The saturations in Tables 2 and 3 were computed from measured specimen weights and dimensions and were particularly sensitive to the specimen thickness, H, which was determined based on the average of four measurements (with calipers) for each specimen. Thus, initial $S > 100\%$ for some of the specimens are attributed to slight errors in H.

Substantial decreases in saturation of all specimens were observed upon drying for all $\Psi_m \geq 50$ kPa, as illustrated in Fig. 5. Saturations after drying were reasonably consistent with those expected based on the SWRCs in Fig. 4, but tended to decrease with increasing cycles. The trend of decreasing saturation with increasing cycles reflects hysteresis in the moisture retention behavior that may have been influenced, at least in part, by volume change that occurred during the cyclic tests (e.g., see Fredlund and Rahardjo 1993). Although the drying cycles did not cause any noticeable lateral shrinkage (i.e., no vertical desiccation cracks through the specimens or sidewall gaps between the edges of the specimens and the retaining rings), a net decrease in thickness was observed in all of the specimens subjected to $\Psi_m \geq 50$ kPa.

For example, average vertical strains for replicate specimens of backfills B1 and B2 are plotted as a function of drying cycle in Fig. 6. Whereas little or no vertical strain (i.e., ≤3%) was observed in the control tests ($\Psi_m = 0$), strains ranging from ~3% to 15% were observed after drying cycles at $\Psi_m \geq 50$ kPa. Strains generally increased with increasing Ψ_m and were slightly greater for specimens of backfill B2 relative to specimens of backfill B1 that were dried at the same Ψ_m. Most of the shrinkage occurred within first two drying cycles, although gradual increases in shrinkage over subsequent drying cycles were observed during tests in which $\Psi_m \geq 150$ kPa. The results in Fig. 6 also illustrate that the shrinkage was not reversed upon rewetting. Rather, slightly greater net shrinkage was measured after each wetting phase relative to the prior drying phase for each cycle. Thus, any swelling of the backfill specimens during rewetting was less than the recompression that occurred under the reapplied load in the consolidometers.

Upon rewetting of the dried specimens ($\Psi_m > 0$), the saturations did not approach 100% after but rather were typically between 70% and 85% (see Fig. 5). Thus, rewetting apparently was insufficient for returning to the saturated (or nearly saturated) condition exhibited by the specimens prior to first drying, despite the fact that several pore volumes of flow (PVF) were passed through most of the test specimens during the permeation stage of rewetting (see Tables 2 and 3). Incomplete saturation upon rewetting likely was due, at least in part, to air entrapment that often occurs when soils are permeated in the absence of backpressure (e.g., Corey 1994; Chiu and Shackelford 1998). Also, although no desiccation cracks or sidewall gaps were observed in any of the specimens, preferential flow along higher-k pathways created during the drying cycles may have contributed to the low S values upon rewetting.

Hydraulic conductivity

Measured k values for replicate backfill specimens in Tables 2 and 3 are plotted as a function of wet–dry cycles in Fig. 7. The trend lines shown in Fig. 7 are fitted through the geometric mean hydraulic conductivity, k_m, for each set of replicates. The k values for each of the three control specimens ($\Psi_m = 0$) of backfill B2 changed minimally over five successive cycles, indicating that the specimen handling procedure had no impact on the hydraulic response of these specimens. Similarly, k values for the two control specimens of backfill B1 also remained stable over the first two cycles.

Table 2. Cyclic drying–wetting test results for consolidated specimens ($\sigma' = 24$ kPa) of backfill B1 (2.7% bentonite). Results for cycle 0 are initial properties (prior to first drying cycle).

Ψ_m (kPa)	Cycle	H (cm)	V (cm³)	e	S (%)	After wetting and permeation					k test duration	
						H (cm)	V (cm³)	e	S (%)	k (cm/s)	t (days)	PVF
0	0	—	—	—	—	2.36	75.6	0.80	98.6	7.3×10^{-8}	13.0	1.88
		—	—	—	—	2.35	76.7	0.81	99.9	7.4×10^{-8}	13.0	1.85
	1	2.36	75.6	0.80	98.6	2.32	75.2	0.79	98.7	7.5×10^{-8}	15.9	2.17
		2.35	76.7	0.81	99.9	2.31	75.9	0.79	100	7.9×10^{-8}	15.9	2.14
	2	2.32	75.2	0.79	98.7	2.29	74.9	0.79	98.7	1.1×10^{-7}	11.9	2.07
		2.31	75.9	0.79	100	2.27	75.8	0.78	99.7	8.6×10^{-8}	11.9	1.96
	3	2.29	74.9	0.79	98.7	2.31	75.6	0.80	97.1	8.4×10^{-7}	10.9	10.6
		2.27	75.8	0.78	99.7	2.33	76.2	0.79	97.9	1.7×10^{-7}	10.9	3.26
	4	2.31	75.6	0.80	97.1	2.27	74.3	0.79	101	1.1×10^{-6}	19.9	21.1
		2.33	76.2	0.79	97.9	2.29	74.6	0.78	103	1.7×10^{-7}	9.8	2.67
50	0	—	—	—	—	2.31	75.5	0.82	99.5	7.1×10^{-8}	7.0	0.56
		—	—	—	—	2.29	74.8	0.80	103	6.3×10^{-8}	7.0	0.52
		—	—	—	—	2.31	75.5	0.83	101	6.5×10^{-8}	7.0	0.51
	1	2.24	73.2	0.77	45.9	2.24	73.2	0.77	83.6	6.6×10^{-8}	21.2	1.61
		2.22	72.5	0.74	46.4	2.22	72.5	0.74	84.6	5.0×10^{-8}	26.1	1.37
		2.27	74.2	0.79	46.4	2.27	74.2	0.79	82.6	5.6×10^{-8}	14.1	1.32
	2	2.23	72.9	0.76	40.6	2.20	71.9	0.74	77.4	1.6×10^{-7}	12.0	3.78
		2.24	73.2	0.76	39.1	2.20	71.9	0.73	80.0	2.7×10^{-7}	12.0	8.29
		2.21	72.2	0.75	45.5	2.16	70.6	0.71	80.1	1.2×10^{-7}	12.0	2.96
	3	2.24	73.2	0.77	34.3	2.14	70.0	0.69	80.3	4.8×10^{-5}	9.1	24.0
		2.24	73.2	0.76	33.9	2.20	71.8	0.72	73.9	1.3×10^{-5}	9.1	23.7
		2.20	71.9	0.74	38.7	2.12	69.2	0.67	81.2	1.3×10^{-5}	9.1	23.0
	4	2.22	72.5	0.75	31.9	2.19	71.5	0.73	73.5	1.2×10^{-5}	10.9	30.9
		2.20	72.0	0.73	31.7	2.17	70.9	0.70	75.9	8.3×10^{-6}	12.2	32.9
		2.19	71.6	0.73	35.3	2.17	70.7	0.71	74.1	5.2×10^{-6}	10.9	31.4
	5	2.19	71.6	0.73	32.8	2.14	70.0	0.69	75.0	7.4×10^{-7}	11.0	20.5
		2.22	72.4	0.74	25.1	2.20	71.7	0.72	71.5	1.4×10^{-6}	11.0	18.1
		2.19	71.6	0.73	30.2	2.16	70.7	0.71	70.9	7.0×10^{-7}	11.0	19.2
150	0	—	—	—	—	2.33	74.9	0.87	99.1	1.1×10^{-7}	7.8	1.50
		—	—	—	—	2.30	74.1	0.84	99.3	1.1×10^{-7}	7.9	1.44
		—	—	—	—	2.34	75.1	0.93	99.4	1.6×10^{-7}	7.8	2.31
	1	2.25	72.4	0.81	23.1	2.18	70.2	0.75	87.2	1.8×10^{-5}	7.1	15.7
		2.26	72.7	0.80	22.6	2.20	70.9	0.76	86.7	1.9×10^{-7}	5.1	1.97
		2.22	71.4	0.83	26.2	2.16	69.5	0.78	99.5	9.7×10^{-7}	5.1	7.05
	2	2.24	72.0	0.80	19.3	2.14	68.8	0.72	83.6	1.3×10^{-4}	5.0	10.7
		2.18	70.2	0.74	19.0	2.11	67.8	0.68	88.6	1.5×10^{-4}	5.0	10.0
		2.16	69.3	0.78	23.2	2.09	67.2	0.72	88.5	2.2×10^{-4}	5.0	11.5
	3	2.19	70.5	0.76	14.8	2.16	69.4	0.73	83.9	2.5×10^{-4}	5.6	15.1
		2.16	69.3	0.72	12.7	2.13	68.5	0.70	85.8	2.4×10^{-4}	5.6	14.8
		2.08	67.0	0.72	18.5	2.05	65.8	0.69	90.5	2.5×10^{-4}	5.6	14.7
400	0	—	—	—	—	2.33	75.8	0.95	95.9	5.3×10^{-8}	9.8	0.49
		—	—	—	—	2.33	75.7	0.92	98.7	5.3×10^{-8}	9.8	0.46
		—	—	—	—	2.29	74.4	0.88	101	5.2×10^{-8}	9.8	0.48
	1	2.18	70.8	0.82	25.3	2.11	68.4	0.76	95.7	7.2×10^{-6}	14.1	30.4
		2.08	67.5	0.72	27.7	2.03	65.8	0.67	107	1.2×10^{-6}	10.1	10.2
		2.13	69.2	0.75	25.7	2.09	67.7	0.72	98.9	2.0×10^{-6}	6.1	10.0
	2	2.18	70.6	0.82	22.6	2.15	69.8	0.79	82.0	3.2×10^{-5}	10.0	13.6
		2.16	70.1	0.78	23.1	2.13	69.1	0.76	78.3	3.1×10^{-5}	10.0	14.9
		2.20	71.3	0.81	21.2	2.17	70.4	0.78	76.6	1.3×10^{-5}	10.0	15.1
	3	2.14	69.4	0.78	20.6	2.12	68.7	0.77	84.9	1.5×10^{-4}	2.9	7.86
		2.12	68.8	0.75	14.4	2.09	67.8	0.72	83.9	8.6×0^{-5}	2.9	8.19
		2.17	70.3	0.78	15.0	2.12	68.9	0.75	77.2	1.2×10^{-5}	2.9	8.17
	4	2.13	69.1	0.78	18.3	2.10	68.3	0.75	86.4	1.3×10^{-4}	2.8	7.53
		2.12	68.8	0.75	18.3	2.10	68.2	0.73	81.0	1.7×10^{-4}	2.8	8.21
		2.15	69.7	0.76	15.5	2.12	68.7	0.74	81.1	8.4×10^{-5}	2.8	8.01
	5	2.08	67.5	0.74	15.8	2.05	66.7	0.71	80.3	2.1×10^{-4}	7.0	16.6
		2.07	67.2	0.71	15.1	2.03	66.0	0.68	94.5	1.9×10^{-4}	7.0	12.2
		2.09	67.7	0.71	14.0	2.07	67.3	0.71	75.0	1.2×10^{-4}	7.0	17.8

Note: Ψ_m, applied matric (drying) suction; H, specimen thickness; V, total volume; e, void ratio; S, degree of saturation; k, hydraulic conductivity; t, time; PVF, pore volumes of flow.

Table 3. Cyclic drying–wetting test results for consolidated specimens ($\sigma' = 24$ kPa) of backfill B2 (5.6% bentonite). Results for cycle 0 are initial properties (prior to first drying cycle).

Ψ_m (kPa)	Cycle	After drying				After wetting and permeation					k test duration	
		H (cm)	V (cm³)	e	S (%)	H (cm)	V (cm³)	e	S (%)	k (cm/s)	t (days)	PVF
0	0	—	—	—	—	2.25	73.4	0.92	101	2.2×10^{-8}	13.0	0.78
		—	—	—	—	2.24	73.3	0.91	99.1	2.2×10^{-8}	13.0	0.55
		—	—	—	—	2.23	74.7	0.92	96.6	2.2×10^{-8}	13.0	0.58
	1	2.25	73.4	0.92	101	2.26	73.6	0.93	99.1	2.1×10^{-8}	15.9	0.63
		2.24	73.3	0.91	99.1	2.23	73.1	0.91	99.2	2.1×10^{-8}	15.9	0.64
		2.23	74.7	0.92	96.6	2.25	73.3	0.91	99.7	2.3×10^{-8}	15.9	0.62
	2	2.26	73.6	0.93	99.1	2.23	72.6	0.90	102	2.1×10^{-8}	11.9	0.45
		2.23	73.1	0.91	99.2	2.19	71.8	0.88	102	2.1×10^{-8}	11.9	0.53
		2.25	73.3	0.91	99.7	2.21	72.0	0.88	103	1.9×10^{-8}	11.9	0.47
	3	2.23	72.6	0.90	102	2.22	72.4	0.89	101	2.1×10^{-8}	10.9	0.42
		2.19	71.8	0.88	102	2.20	71.9	0.88	101	2.2×10^{-8}	10.9	0.45
		2.21	72.0	0.88	103	2.23	72.6	0.89	100	1.7×10^{-8}	10.9	0.38
	4	2.22	72.4	0.89	101	2.19	71.2	0.88	101	1.9×10^{-8}	11.8	0.43
		2.20	71.9	0.88	101	2.20	72.0	0.88	101	2.6×10^{-8}	11.8	0.63
		2.23	72.6	0.89	100	2.19	71.2	0.86	103	1.5×10^{-8}	11.8	0.39
50	0	—	—	—	—	2.26	73.4	0.94	100	2.1×10^{-8}	7.9	0.21
		—	—	—	—	2.27	73.8	0.97	103	2.3×10^{-8}	7.9	0.36
		—	—	—	—	2.16	70.0	0.85	111	2.2×10^{-8}	7.9	0.23
	1	2.20	71.4	0.89	62.3	2.17	70.3	0.86	86.6	1.1×10^{-8}	27.9	0.82
		2.19	71.2	0.90	52.2	2.11	68.4	0.83	94.1	1.4×10^{-8}	27.9	0.55
		2.15	69.7	0.84	62.2	2.06	66.8	0.76	99.3	1.2×10^{-8}	27.9	0.87
	2	2.05	66.6	0.76	75.2	2.01	65.4	0.73	99.0	8.9×10^{-9}	16.3	0.42
		2.08	67.5	0.80	82.2	2.04	66.4	0.77	98.2	8.0×10^{-9}	16.3	0.24
		2.06	66.9	0.77	76.0	2.01	65.4	0.73	95.3	6.2×10^{-9}	16.3	0.19
	3	2.11	68.5	0.81	54.0	2.08	67.6	0.79	79.4	1.5×10^{-8}	13.0	0.45
		2.11	68.5	0.83	57.8	2.07	67.1	0.79	83.7	1.1×10^{-5}	14.0	20.7
		2.08	67.5	0.78	79.0	2.02	65.5	0.73	89.4	7.6×10^{-9}	13.0	0.25
	4	2.09	67.7	0.79	50.4	2.01	65.2	0.72	82.1	2.3×10^{-8}	7.2	0.55
		2.11	68.4	0.83	50.1	2.06	66.9	0.79	79.0	2.3×10^{-5}	8.0	15.5
		2.07	67.1	0.77	63.8	2.05	66.5	0.76	80.3	9.5×10^{-9}	8.0	0.22
	5	2.08	67.5	0.78	47.9	1.96	63.6	0.68	85.3	1.1×10^{-5}	10.1	24.3
		2.06	66.8	0.78	48.1	2.03	65.8	0.76	78.8	7.4×10^{-5}	10.1	21.4
		2.05	66.6	0.76	62.2	1.99	64.6	0.70	82.5	2.2×10^{-8}	7.0	0.54
	6	2.06	66.7	0.76	36.8	2.01	65.1	0.72	80.2	1.1×10^{-7}	7.0	2.32
		2.08	67.4	0.80	36.2	2.05	66.5	0.78	76.9	1.0×10^{-5}	9.0	22.6
		2.05	66.7	0.76	44.4	2.03	65.8	0.74	75.6	2.2×10^{-8}	7.0	0.44
	7	2.08	67.5	0.78	40.1	1.94	63.0	0.67	87.2	3.0×10^{-7}	10.1	10.6
		2.07	67.3	0.80	32.5	2.05	66.6	0.78	74.9	1.4×10^{-5}	9.1	14.2
		2.06	66.7	0.76	43.5	1.99	64.8	0.71	77.5	3.2×10^{-8}	10.1	0.78
400	0	—	—	—	—	2.26	73.7	1.00	96.7	1.9×10^{-8}	7.9	0.22
		—	—	—	—	2.27	74.3	0.99	101	2.2×10^{-8}	7.9	0.24
		—	—	—	—	2.26	73.7	1.00	99.6	2.0×10^{-8}	7.9	0.38
	1	2.13	69.6	0.89	26.0	2.08	67.9	0.84	86.0	1.3×10^{-8}	35.0	8.97
		2.14	69.9	0.87	23.5	2.09	68.1	0.82	84.6	6.8×10^{-9}	31.6	0.48
		2.15	70.3	0.91	24.4	2.09	68.4	0.86	87.0	1.4×10^{-8}	35.0	1.04
	2	2.09	68.3	0.85	22.4	2.06	67.2	0.83	75.0	1.3×10^{-5}	14.0	22.8
		2.09	68.3	0.83	25.0	2.06	67.4	0.80	83.1	8.4×10^{-9}	13.0	0.32
		2.11	68.9	0.87	21.8	2.05	67.1	0.82	74.2	7.1×10^{-6}	14.0	20.6
	3	2.03	66.2	0.80	20.7	1.99	65.0	0.77	81.2	3.1×10^{-5}	4.9	12.7
		2.05	66.9	0.79	20.3	2.01	65.6	0.75	75.4	1.2×10^{-5}	14.7	5.85
		2.05	67.1	0.82	19.9	2.00	65.4	0.78	82.5	8.4×10^{-5}	11.9	24.0
	4	2.01	65.7	0.78	19.7	2.00	65.2	0.77	76.2	1.1×10^{-4}	7.0	17.1
		2.05	67.0	0.79	19.0	1.99	65.0	0.74	79.8	1.0×10^{-5}	7.0	16.2
		2.03	66.2	0.80	19.5	2.00	65.2	0.77	76.2	7.8×10^{-5}	7.0	17.1
	5	2.00	65.4	0.78	17.1	1.96	64.0	0.74	79.7	3.2×10^{-4}	8.0	20.0
		1.98	64.5	0.73	25.7	1.93	63.2	0.69	85.5	4.0×10^{-5}	8.0	19.5
		1.98	64.7	0.76	16.2	1.94	63.4	0.72	81.5	1.4×10^{-4}	8.0	20.4

Table 3 (*concluded*).

Ψ_m (kPa)	Cycle	After drying				After wetting and permeation					k test duration	
		H (cm)	V (cm³)	e	S (%)	H (cm)	V (cm³)	e	S (%)	k (cm/s)	t (days)	PVF
700	0	—	—	—	—	2.28	74.0	1.10	101	2.2×10^{-8}	7.7	0.18
		—	—	—	—	2.34	75.9	1.05	93.3	2.2×10^{-8}	10.0	0.23
		—	—	—	—	2.36	76.8	1.05	94.9	2.4×10^{-8}	10.0	0.23
	1	2.16	70.1	1.00	24.3	2.09	67.7	0.93	87.6	7.7×10^{-7}	9.0	7.90
		2.12	68.8	0.86	18.4	2.03	66.0	0.79	94.8	4.1×10^{-8}	29.8	2.14
		2.10	68.2	0.82	23.7	2.00	65.0	0.74	103	9.4×10^{-9}	32.9	0.49
	2	2.03	65.9	0.88	21.5	1.99	64.6	0.84	85.5	4.2×10^{-5}	12.9	20.3
		2.06	66.9	0.81	18.4	2.01	65.4	0.77	70.1	8.8×10^{-6}	12.9	25.6
		2.10	68.2	0.82	19.2	2.05	66.5	0.77	64.4	9.8×10^{-8}	12.9	3.15
	3	1.98	64.3	0.83	18.7	1.93	62.7	0.79	85.0	6.9×10^{-5}	5.1	14.5
		2.06	66.9	0.81	16.1	2.00	64.9	0.76	75.5	1.3×10^{-6}	6.1	13.5
		2.05	66.6	0.78	18.1	1.96	63.7	0.70	85.8	1.1×10^{-5}	6.1	17.2
	4	1.96	63.6	0.81	17.5	1.85	60.0	0.71	91.2	1.7×10^{-4}	6.8	16.6
		2.08	67.5	0.83	14.3	2.05	66.7	0.80	70.9	7.7×10^{-5}	6.8	16.2
		2.05	66.6	0.78	16.5	2.03	65.8	0.76	76.8	7.5×10^{-5}	6.8	16.0
	5	1.93	62.5	0.78	13.4	1.86	60.3	0.72	96.4	2.2×10^{-4}	6.8	14.7
		2.07	67.1	0.81	12.5	2.04	66.2	0.79	74.4	2.3×10^{-4}	6.8	17.1
		2.03	65.8	0.76	15.3	1.91	62.1	0.66	84.9	1.5×10^{-4}	6.8	18.0

Note: Ψ_m, applied matric (drying) suction; H, specimen thickness; V, total volume; e, void ratio; S, degree of saturation; k, hydraulic conductivity; t, time; PVF, pore volumes of flow.

Fig. 5. Saturations for replicate specimens of backfills B1 (2.7% bentonite) and B2 (5.6% bentonite) after drying and after wetting, as a function of the number of wet–dry cycles and the matric suction (Ψ_m) applied during the drying phase. Open symbols, after drying; closed symbols, after wetting.
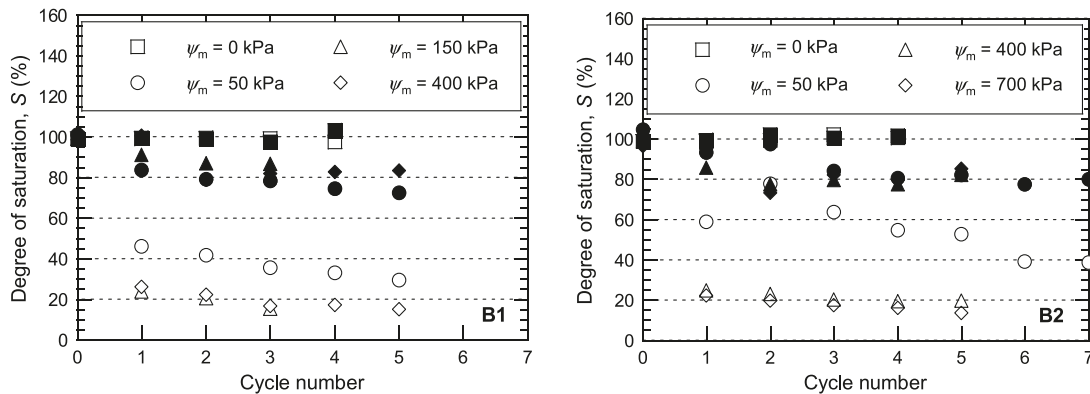

Slight increases in k (an order of magnitude or less) were exhibited by these specimens after the third cycle.

In contrast to the control specimens, k values for the dried specimens ($\Psi_m \geq 50$ kPa) ranged over several orders of magnitude (i.e., between 10^{-8} and 10^{-3} cm/s), depending upon the number of cycles and the applied Ψ_m during the drying phase. The greatest increases in k were observed for specimens dried at $\Psi_m \geq 150$ kPa for backfill B1 and $\Psi_m \geq 400$ kPa for backfill B2. In these tests, k typically increased after one or two cycles and continued to increase until k was between 10^{-3} and 10^{-5} cm/s after 3–5 cycles. The large increases in k observed for specimens of both backfills after drying at high Ψ_m were reasonably consistent among replicates, particularly after the third cycle. In addition, the consistently high k exhibited by the specimens after successive cycles indicate that the degradation in k caused by drying at high Ψ_m was not reversible, even after passing several PVF through the specimens during permeation (typically 8–30 PVF for specimens with $k > 10^{-6}$ cm/s; see Tables 2 and 3).

Specimens dried at $\Psi_m = 50$ kPa exhibited little or no change in k after two cycles and generally demonstrated greater resiliency after three or more cycles than specimens dried at $\Psi_m \geq 150$ kPa. For example, k of each replicate specimen of backfill B1 increased by approximately two orders of magnitude after the third drying cycle, but subsequently decreased to within one order of magnitude of the initial k after the fifth drying cycle. In the case of backfill B2, measured k values for two of the three replicate specimens (i.e., specimens A and C) remained stable through four drying cycles and were within one order of magnitude of the initial k after seven drying cycles. Only specimen B of backfill B2 exhibited a consistent inability to heal after three or more cycles of drying at $\Psi_m = 50$ kPa.

The trends in Fig. 7 indicate that backfill B1 (2.7% bentonite) generally exhibited greater susceptibility to increases in k after drying than backfill B2 (5.6% bentonite). Although both backfills exhibited a consistently stable hydraulic response after two drying cycles at $\Psi_m = 50$ kPa, all three

Fig. 6. Cumulative vertical strains (average of replicates) for specimens of backfills B1 and B2 after the drying and wetting phase of each wet–dry cycle.
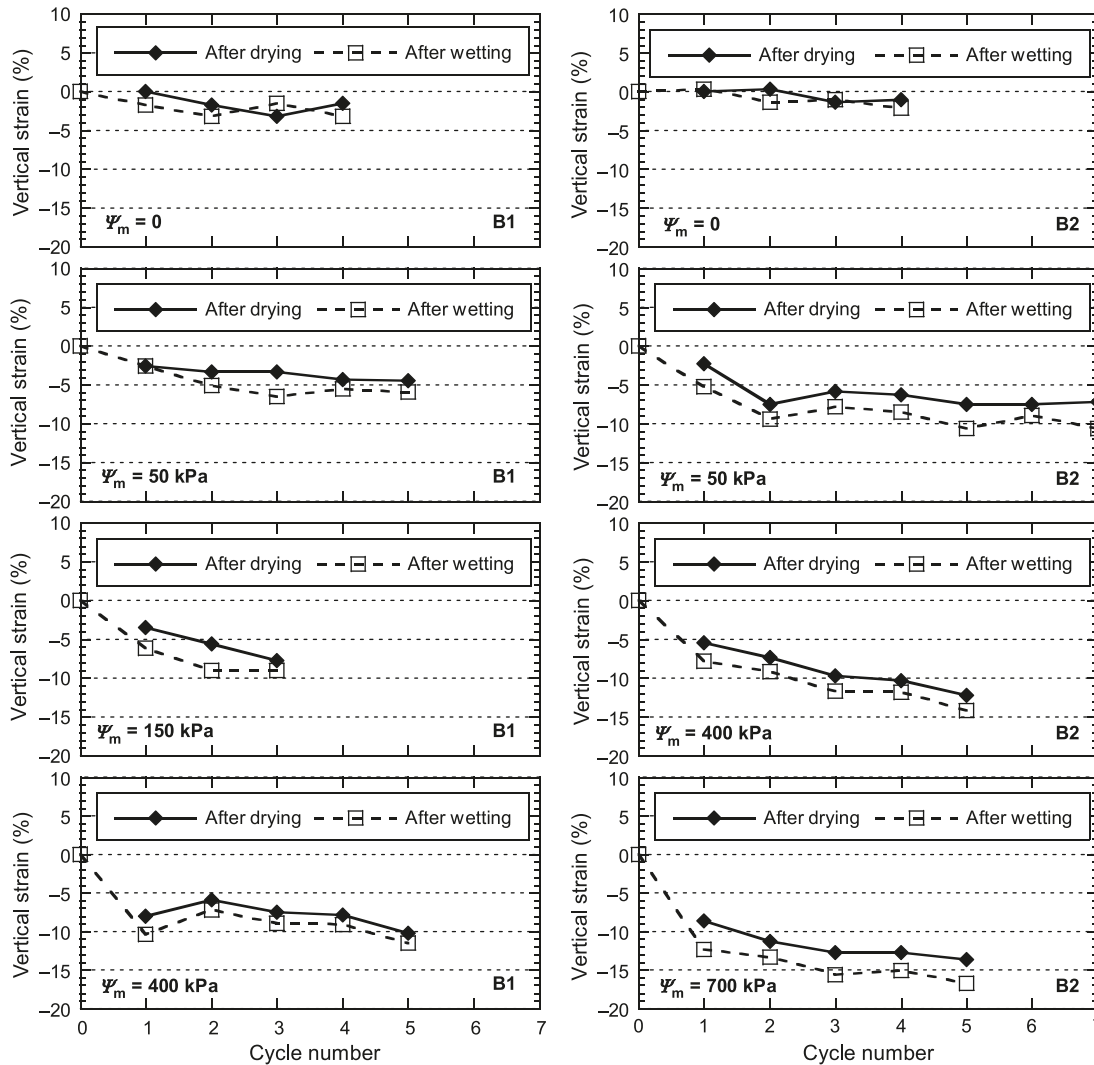
specimens of backfill B1 exhibited an ~300-fold increase in k after the third drying cycle at $\Psi_m = 50$ kPa. In contrast, k for two of the three replicate specimens of backfill B2 (i.e., specimens A and C) remained stable for at least two additional cycles. The variability in k_m of replicate specimens of backfill B2 after three or more cycles of drying at $\Psi_m = 50$ kPa is largely due to the high k of one of the three replicates (specimen B). Moreover, five of the six specimens of backfill B1 that were dried at $\Psi_m \geq 150$ kPa exhibited ~10-fold or greater increases in k after one drying cycle, whereas only one specimen of backfill B2 dried at $\Psi_m \geq 400$ kPa exhibited a 10-fold or greater increase in k after one drying cycle.

The hydraulic conductivities in Fig. 7 are consistent with the saturation and strain data in Figs. 5 and 6 in that greater degradation in k occurred for specimens that experienced greater desaturation and shrinkage upon drying. For example, values of k_m corresponding to the fitted trend lines in Fig. 7 were normalized with respect to the initial k_m prior to first

drying (i.e., $k_{m,o}$), and the resulting values of the ratio $k_m/k_{m,o}$ are plotted as a function of the number of wet–dry cycles in Fig. 8. For the four sets of replicate specimens dried at $\Psi_m \geq 150$ kPa, $k_m/k_{m,o}$ followed similar, increasing trends with successive cycles and ranged from ~500 to 10 000 after three or more cycles. These four sets of specimens all exhibited $S < 30\%$ after drying and net vertical shrinkage of up to 17% over the course of the tests (see Figs. 5 and 6). In contrast, the two sets of specimens dried at $\Psi_m = 50$ kPa exhibited greater saturations after drying (typically 30%–60%), less vertical shrinkage (typically <10%), and lower values of $k_m/k_{m,o}$ after three or more cycles (~5–300).

Based on the findings above, increases in k due to wet–dry cycling may be a concern for sandy SB backfills in which k is governed by the bentonite fraction in the backfill. In order for such backfills to maintain a low k, the bentonite must be able to plug the larger voids between the sand particles effectively. The large increases in k of the specimens indicate that large pores became available for flow, despite the net vertical

Fig. 7. Hydraulic conductivities (*k*) for replicate specimens A, B, and C of backfills B1 (2.7% bentonite) and B2 (5.6% bentonite) subjected to wet–dry cycles (trend lines are drawn through the geometric mean *k* of replicates).
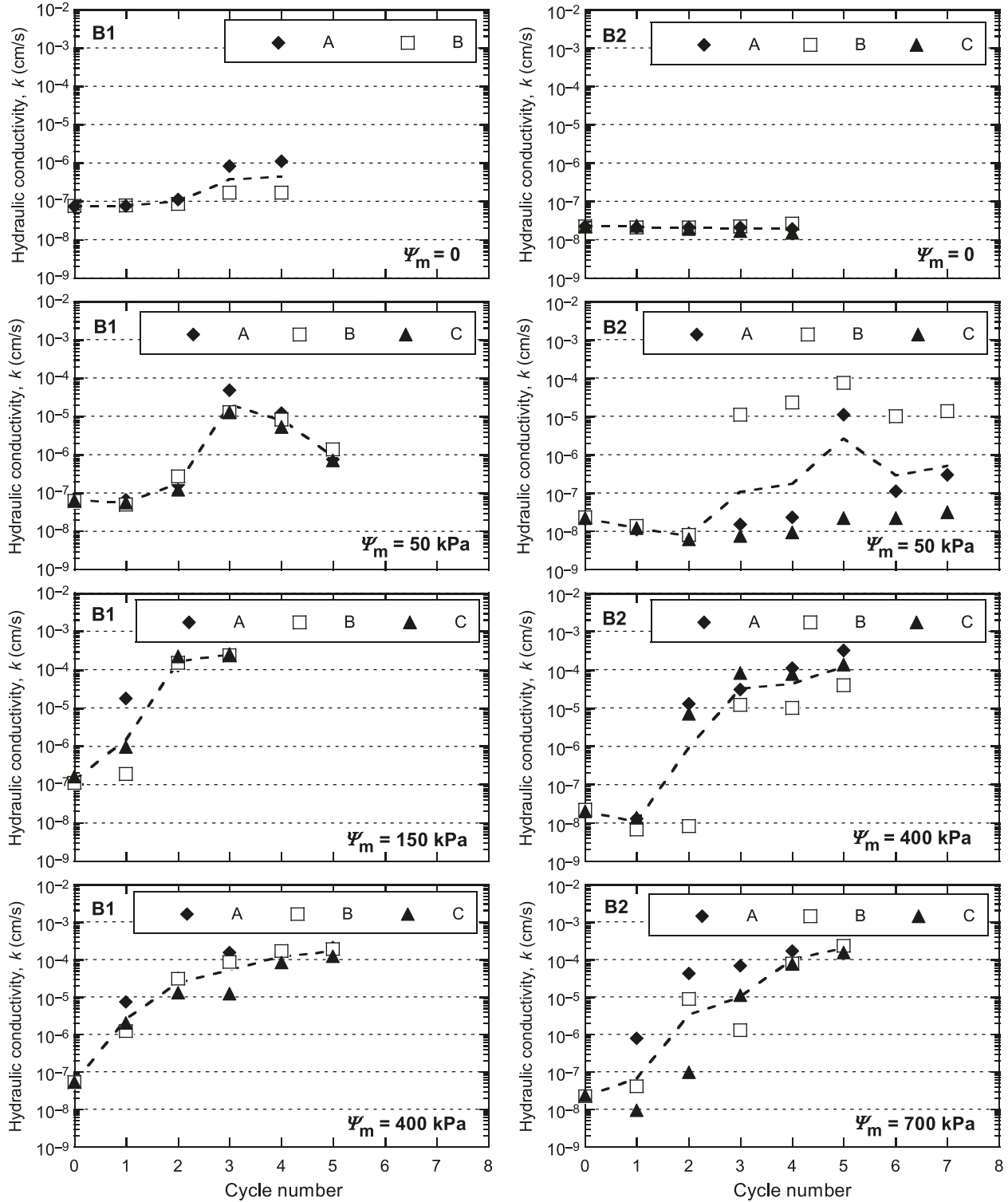

compression exhibited by the specimens. Also, the relatively low saturations upon rewetting (see Fig. 5) suggest that large, unplugged voids may have acted as preferential flow paths in the specimens. Such voids can develop in sand–bentonite mixtures due to suffosion (internal erosion) of the bentonite, a process that has been reported as a potential concern for compacted sand–bentonite liners (e.g., Chapuis 2002). However, large increases in *k* due to suffosion in laboratory tests generally coincide with tail water turbidity that reflects the presence of bentonite in the outflow (e.g., Marcotte et al. 1994; Chapuis et al. 2006). Turbid tail water was not observed in any of the tests conducted in this study.

Fig. 8. Ratios of geometric mean hydraulic conductivity (k_m) to initial geometric mean hydraulic conductivity ($k_{m,o}$) for replicate specimens of backfills B1 and B2 as a function of wet–dry cycles and matric suction (Ψ_m) applied during the drying phase.
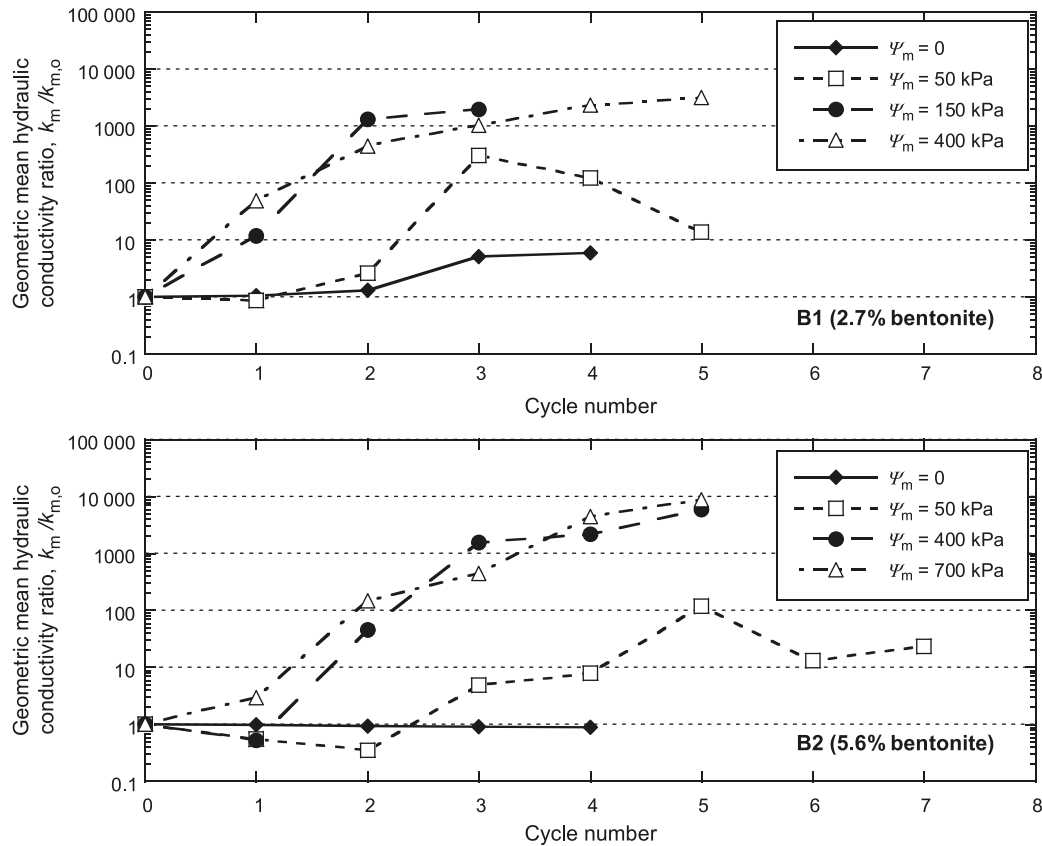
While no prior studies have been performed to evaluate the influence of wet–dry cycling on k of SB backfills, the increases in k shown in Figs. 7 and 8 are consistent with those reported for GCLs that have experienced dehydration (e.g., Egloffstein 2001; Meer and Benson 2007; Benson and Meer 2009; Mazzieri 2011; Scalia and Benson 2011). In these studies, the increases in k were attributed, at least in part, to diminished swelling capacity of the bentonite caused by replacement of exchangeable Na^+ with divalent cations (e.g., Ca^{2+} and Mg^{2+}). For example, Benson and Meer (2009) reported a 100 000-fold increase in k of a GCL specimen after six wet–dry cycles with a solution having a low ionic strength ($I = 0.005$ mol/L) but containing an abundance of Ca^{2+} relative to Na^+ (i.e., relative abundance of monovalent and divalent cations, $RMD = M_m/M_d^{1/2} = 0.007$, where M_m and M_d are the molar concentrations of monovalent and divalent species, respectively). Moreover, the specimen was not able to heal after three additional cycles. Subsequent analysis of the GCL bentonite revealed that nearly all of the Na^+ on the original exchange complex of the bentonite had been replaced by Ca^{2+}.

The final exchange complex of the bentonite in the backfill specimens was not analyzed in this study. Therefore, no definitive conclusions can be made regarding the influence of cation exchange on the trends in Figs. 7 and 8. However, the tap water used in this study exhibited a similar ionic strength ($I = 0.0028$ mol/L) as the solution described above that was used by Benson and Meer (2009) and contained predominantly divalent cations Ca^{2+} and Mg^{2+} ($M_d = 0.0006$ mol/L;

$M_m = 0.0004$ mol/L; $RMD = 0.016$). In addition, the backfill specimens contained only a small fraction of bentonite (<6%), and nearly all of the remaining solids were inert (sand). Thus, less exchange may be necessary to induce large increases in k of the backfills relative to GCLs. Finally, the tap water served as both the wetting and permeant water in the cyclic tests and the base water for the slurry used to create the bulk backfill mixtures. As a result, some cation exchange likely had occurred in the backfills before the test specimens were prepared. Further investigation into the influence of cation exchange on the degradation in k of SB backfills subjected to wet–dry cycling is warranted based on these considerations.

From a practical standpoint, the findings of this study suggest that wet–dry cycling could possibly contribute to degradation in the containment performance of SB vertical barriers in the zone of a fluctuating water table. However, the significance of such an impact would depend on various site-specific conditions, including the length of the portion of the barrier subjected to wet–dry cycling, the number of drying cycles, and any of several factors that influence the matric suction profile and extent of drying with depth and over time (e.g., the hydraulic and moisture retention properties of the backfill and surrounding soils, the depth to the water table, the thickness of the root zone, and climatic conditions). Moreover, the backfill compositions and range of matric suctions considered in this study are not representative of the entire range of possible field conditions for vertical barriers. For example, backfills that contain less bentonite and more

native fines than the model backfills tested in this study may exhibit markedly different water retention characteristics and may respond differently to wet–dry cycling. Also, matric suctions ≥50 kPa likely would develop within only a portion of the potential desiccation zone in a vertical barrier such as illustrated in Fig. 1. Additional testing of backfills with different compositions and subjected to drying at matric suctions <50 kPa is needed to capture a wider range of possible field conditions.

Summary and conclusions

The purpose of this study was to evaluate the potential for changes in hydraulic conductivity (k) of two model SB backfills subjected to wet–dry cycling, with tap water used as the wetting and permeant liquid. The backfills were prepared using clean sand as the base soil, but each backfill contained a different dry weight percentage of bentonite (2.7% and 5.6%, respectively). Saturation, volume change, and the hydraulic response exhibited by consolidated specimens ($\sigma' = 24$ kPa) of the backfills were evaluated over 3–7 wet–dry cycles in which the applied matric suction during the drying phase ranged from 50 to 700 kPa. Soil-water retention (drying) curves also were measured independently for each backfill and were fitted with the van Genuchten model.

The results of the wet–dry tests showed that significant increases in k occurred for specimens of both backfills after cyclic drying under high matric suctions (≥150 kPa) that resulted in saturations <30%. In these tests, the geometric mean hydraulic conductivity, k_m, of replicate specimens containing 2.7% bentonite increased from ≤10^{-7} cm/s before first drying to ≥10^{-6} cm/s after the first drying cycle, whereas k_m of specimens containing 5.6% bentonite remained below 10^{-7} cm/s after one drying cycle. However, both backfills exhibited 500-fold to 10 000-fold increases in k_m after three or more drying cycles, and the specimens did not heal even after long periods of permeation. Specimens dried to a lesser extent (saturations of 30%–60%) exhibited a stable hydraulic response after two drying cycles and generally were more resilient than specimens dried to saturations <30%, although fivefold to 300-fold increases in k_m were observed for specimens of both backfills after three or more cycles. In contrast, values of k_m for control (undried) specimens, though subjected to the same cyclic handling procedure as the dried specimens, remained within one order of magnitude of the initial k_m over five successive cycles.

Additional research is necessary to elucidate the mechanisms responsible for the large increases in k observed in this study. In particular, the potential significance of cation exchange in the bentonite upon exposure to divalent cations during backfill preparation and permeation warrants further investigation. Moreover, backfills containing different soil compositions and subjected to less drying than the model backfills tested in this study may respond differently to wet–dry cycling. Thus, future studies are needed to investigate a wider range of backfill compositions and matric suctions lower than those used in this study (50–700 kPa). Nonetheless, the findings illustrate the potential for increases in hydraulic conductivity to occur for SB backfills subjected to wet–dry cycling. The extent to which such degradation may affect the overall containment performance of a constructed barrier will depend upon site-specific factors, such as the length of the portion of the barrier subjected to cyclic drying, the number of wet–dry cycles, and the extent of drying that occurs in the backfill during each cycle. The water retention characteristics (i.e., van Genuchten fitting parameters) reported herein may be useful for incorporation into an unsaturated flow model to predict the matric suction profile and corresponding saturations in constructed barriers with similar backfill compositions based on site-specific conditions.

Acknowledgements

References

Abichou, T., Benson, C.H., and Edil, T.B. 2000. Foundry green sands as hydraulic barriers: laboratory study. Journal of Geotechnical and Geoenvironmental Engineering, **126**(12): 1174–1183. doi:10.1061/(ASCE)1090-0241(2000)126:12(1174).

Albrecht, B.A., and Benson, C.H. 2001. Effect of desiccation on compacted natural clays. Journal of Geotechnical and Geoenvironmental Engineering, **127**(1): 67–75. doi:10.1061/(ASCE)1090-0241(2001)127:1(67).

Andromalos, K.B., and Fisher, M.J. 2001. Design and control of slurry wall backfill mixes for groundwater containment. *In* Proceedings of the International Containment and Remediation Technology Conference, Orlando, Fla., 10–13 June 2001. Florida State University, Tallahassee, Fla.

ASTM. 2007. Standard test method for particle size analysis of soils. ASTM standard D422-63(2007). *In* Annual Book of ASTM Standards, Vol. 04.08. American Society for Testing and Materials (ASTM) International, West Conshohocken, Pa. doi:10.1520/D0422-63R07.

ASTM. 2008. Standard test methods for determination of the soil water characteristic curve for desorption using a hanging column, pressure extractor, chilled mirror hygrometer, and/or centrifuge. ASTM standard D6836-02(2008)e2. *In* Annual Book of ASTM Standards, Vol. 04.09. American Society for Testing and Materials (ASTM) International, West Conshohocken, Pa. doi:10.1520/D6836-02R08E02.

ASTM. 2010*a*. Standard practice for classification of soils for engineering purposes (Unified Soil Classification System). ASTM standard D2487-10. American Society for Testing and Materials (ASTM) International, West Conshohocken, Pa. doi:10.1520/D2487-10.

ASTM. 2010*b*. Standard test methods for liquid limit, plastic limit, and plasticity index of soils. ASTM standard D4318-10. *In* Annual Book of ASTM Standards, Vol. 04.08. American Society for Testing and Materials (ASTM) International, West Conshohocken, Pa. doi:10.1520/D4318-10.

ASTM. 2010*c*. Standard test method for slump of hydraulic-cement concrete. ASTM standard C143/C143M-10. American Society for Testing and Material (ASTM) International, West Conshohocken, Pa. doi:10.1520/C0143_C0143M-10.

Benson, C., and Meer, S. 2009. Relative abundance of monovalent

and divalent cations and the impact of desiccation on geosynthetic clay liners. Journal of Geotechnical and Geoenvironmental Engineering, **135**(3): 349–358. doi:10.1061/(ASCE)1090-0241 (2009)135:3(349).

Boardman, B.T., and Daniel, D.E. 1996. Hydraulic conductivity of desiccated geosynthetic clay liners. Journal of Geotechnical Engineering, **122**(3): 204–208. doi:10.1061/(ASCE)0733-9410 (1996)122:3(204).

Chapuis, R.P. 2002. Full-scale hydraulic performance of soil–bentonite and compacted clay liners. Canadian Geotechnical Journal, **39**(2): 417–439. doi:10.1139/t01-092.

Chapuis, R.P., Marcotte, D., and Aubertin, M. 2006. Discussion of "Network model for hydraulic conductivity of sand–bentonite mixtures". Canadian Geotechnical Journal, **43**(1): 110–114. doi:10.1139/t05-074.

Chiu, T.-F., and Shackelford, C.D. 1998. Unsaturated hydraulic conductivity of compacted sand–kaolin mixtures. Journal of Geotechnical and Geoenvironmental Engineering, **124**(2): 160–170. doi:10.1061/(ASCE)1090-0241(1998)124:2(160).

Corey, A. 1994. Mechanics of immiscible fluids in porous media. Water Resources Publications, Highlands Ranch, Colo.

D'Appolonia, D.J. 1980. Soil–bentonite slurry trench cutoffs. Journal of the Geotechnical Engineering Division, ASCE, **106**(4): 399–417.

Egloffstein, T. 2001. Natural bentonites — influence of the ion exchange and partial desiccation on permeability and self-healing capacity of bentonites used in GCLs. Geotextiles and Geomembranes, **19**(7): 427–444. doi:10.1016/S0266-1144(01)00017-6.

Evans, J.C. 1993. Vertical cutoff walls. *In* Geotechnical practice for waste disposal. *Edited by* D.E. Daniel. Chapman and Hall, London, U.K. pp. 430–454.

Evans, J.C. 1994. Hydraulic conductivity of vertical cutoff walls. *In* Hydraulic conductivity and waste contaminant transport in soils, ASTM STP 1142. *Edited by* D.E. Daniel and S.J. Trautwein. American Society for Testing and Materials (ASTM) International, Philadelphia, Pa. pp. 79–94.

Evans, J.C. 1995. Soil- and cement-based vertical barriers with focus on materials. *In* Assessment of barrier containment technologies — a comprehensive treatment for environmental applications. *Edited by* R. Rumer and J. Mitchell. U.S. Department of Energy, U.S. Environmental Protection Agency, Dupont Co., Baltimore, Md. pp. 5–43.

Filz, G.M., Evans, J.C., and Britton, J.P. 2003. Soil–bentonite hydraulic conductivity: measurement and variability. *In* Proceedings of the 12th PanAmerican Conference on Soil Mechanics and Geotechnical Engineering, Cambridge, Mass., 22–26 June 2003. *Edited by* P.J. Culligan, H.H. Einstein, and A.J. Whittle. Verlag Glückauf GMBH (VGE), Essen, Germany. pp. 1323–1328.

Fredlund, D.G., and Rahardjo, H. 1993. Soil mechanics for unsaturated soils. Wiley, New York, N.Y.

Hewitt, R.D., and Daniel, D.E. 1997. Hydraulic conductivity of geosynthetic clay liners after freeze–thaw. Journal of Geotechnical and Geoenvironmental Engineering, **123**(4): 305–313. doi:10.1061/(ASCE)1090-0241(1997)123:4(305).

Jo, H.Y., Benson, C.H., Shackelford, C.D., Lee, J.-M., and Edil, T.B. 2005. Long-term hydraulic conductivity of a geosynthetic clay liner permeated with inorganic salt solutions. Journal of Geotechnical and Geoenvironmental Engineering, **131**(4): 405–417. doi:10.1061/(ASCE)1090-0241(2005)131:4(405).

Jo, H.Y., Benson, C.H., and Edil, T.B. 2006. Rate-limited cation exchange in thin bentonitic barrier layers. Canadian Geotechnical Journal, **43**(4): 370–391. doi:10.1139/t06-014.

Kolstad, D.C., Benson, C.H., and Edil, T.B. 2004a. Hydraulic conductivity and swell of nonprehydrated geosynthetic clay liners permeated with multispecies inorganic solutions. Journal of Geotechnical and Geoenvironmental Engineering, **130**(12): 1236–1249. doi:10.1061/(ASCE)1090-0241(2004)130:12(1236).

Kolstad, D.C., Benson, C.H., Edil, T.B., and Jo, H.Y. 2004b. Hydraulic conductivity of a dense prehydrated GCL permeated with aggressive inorganic solutions. Geosynthetics International, **11**(3): 233–241.

Kraus, J.F., Benson, C.H., Erickson, A.E., and Chamberlain, E.J. 1997. Freeze–thaw cycling and hydraulic conductivity of bentonitic barriers. Journal of Geotechnical and Geoenvironmental Engineering, **123**(3): 229–238. doi:10.1061/(ASCE)1090-0241(1997)123:3(229).

LaGrega, M.L., Buckingham, P.L., and Evans, J.C. 2001. Hazardous waste management, 2nd ed. McGraw-Hill Book Company, New York, N.Y.

Lin, L.C., and Benson, C.H. 2000. Effect of wet–dry cycling on swelling and hydraulic conductivity of GCLs. Journal of Geotechnical and Geoenvironmental Engineering, **126**(1): 40–49. doi:10.1061/(ASCE)1090-0241(2000)126:1(40).

Malusis, M.A., Evans, J.C., McLane, M.H., and Woodward, N.R. 2008. A miniature cone for measuring the slump of soil–bentonite slurry trench cutoff wall backfill. Geotechnical Testing Journal, **31**(5): 373–380.

Malusis, M.A., Barben, E.J., and Evans, J.C. 2009. Hydraulic conductivity and compressibility of a model soil–bentonite backfill amended with activated carbon. Journal of Geotechnical and Geoenvironmental Engineering, **135**(5): 664–672. doi:10.1061/(ASCE)GT.1943-5606.0000041.

Marcotte, D., Marron, J.C., and Fafard, M. 1994. Washing of bentonite in laboratory hydraulic conductivity tests. Journal of Environmental Engineering, **120**(3): 691–698. doi:10.1061/(ASCE)0733-9372(1994)120:3(691).

Mazzieri, F. 2011. Impact of desiccation and cation exchange on the hydraulic conductivity of factory-prehydrated GCLs. *In* GeoFrontiers 2011: Advances in Geotechnical Engineering, Dallas, Tex., 13–16 March 2011. GSP 211. [CD-ROM]. *Edited by* J. Han and D.A. Alzamora. American Society of Civil Engineers, Reston, Va. pp. 976–985.

Meer, S., and Benson, C. 2007. Hydraulic conductivity of geosynthetic clay liners exhumed from landfill final covers. Journal of Geotechnical and Geoenvironmental Engineering, **133**(5): 550–563. doi:10.1061/(ASCE)1090-0241(2007)133:5(550).

National Research Council. 2007. Assessment of the performance of engineered waste containment facilities. The National Academies Press, Washington, D.C.

Othman, M., and Benson, C. 1993. Effect of freeze–thaw on the hydraulic conductivity and morphology of compacted clay. Canadian Geotechnical Journal, **30**(2): 236–246. doi:10.1139/t93-020.

Owaidat, L.M., Andromalos, K.B., and Sisley, J.L. 1999. Construction of a soil–cement–bentonite slurry wall for a levee strengthening program. *In* Proceedings of the 1999 Annual Conference of the Association of State Dam Safety Officials, St. Louis, Mo., 10–13 October 1999. Association of State Dam Safety Officials, Lexington, Ky.

Petrov, R.J., and Rowe, R.K. 1997. Geosynthetic clay liner (GCL) – chemical compatibility by hydraulic conductivity testing and factors impacting its performance. Canadian Geotechnical Journal, **34**(6): 863–885. doi:10.1139/t97-055.

Petrov, R.J., Rowe, R.K., and Quigley, R.M. 1997. Selected factors influencing GCL hydraulic conductivity. Journal of Geotechnical and Geoenvironmental Engineering, **123**(8): 683–695. doi:10.1061/(ASCE)1090-0241(1997)123:8(683).

Podgorney, R.K., and Bennett, J.E. 2006. Evaluating the long-term

performance of geosynthetic clay liners exposed to freeze–thaw. Journal of Geotechnical and Geoenvironmental Engineering, **132**(2): 265–268. doi:10.1061/(ASCE)1090-0241(2006)132:2(265).

Ruffing, D.G., Evans, J.C., and Malusis, M.A. 2010. Prediction of earth pressures in soil–bentonite cutoff walls. *In* GeoFlorida 2010: Advances in Analysis, Modeling, and Design, West Palm Beach, Fla., 20–24 February 2010. *Edited by* D.O. Fratta, A.J. Puppala, and B. Muhunthan. GSP 199. American Society of Civil Engineers, Reston, Va. pp. 2416–2425.

Scalia, J., and Benson, C. 2010. Preferential flow in geosynthetic clay liners exhumed from final covers with composite barriers. Canadian Geotechnical Journal, **47**(10): 1101–1111. doi:10.1139/T10-018.

Scalia, J., and Benson, C. 2011. Hydraulic conductivity of geosynthetic clay liners exhumed from landfill final covers with composite barriers. Journal of Geotechnical and Geoenvironmental Engineering, **137**(1): 1–13. doi:10.1061/(ASCE)GT.1943-5606.0000407.

Shackelford, C.D., and Jefferis, S.A. 2000. Geoenvironmental engineering for in situ remediation. *In* Proceedings of the International Conference on Geotechnical and Geoenvironmental Engineering (GeoEng2000), Melbourne, Australia, 19–24 November 2000. Technomic Publishing Co., Lancaster, Pa. pp. 121–185.

Shackelford, C., Benson, C., Katsumi, T., Edil, T., and Lin, L. 2000. Evaluating the hydraulic conductivity of GCLs permeated with non-standard liquids. Geotextiles and Geomembranes, **18**(2–4): 133–161. doi:10.1016/S0266-1144(99)00024-2.

Sharma, H.D., and Reddy, K.R. 2004. Geoenvironmental engineering. Wiley, Hoboken, N.J.

Southen, J.M., and Rowe, R.K. 2005. Laboratory investigation of geosynthetic clay liner desiccation in a composite liner subjected to thermal gradients. Journal of Geotechnical and Geoenvironmental Engineering, **131**(7): 925–935. doi:10.1061/(ASCE)1090-0241(2005)131:7(925).

Stern, R.T., and Shackelford, C.D. 1998. Permeation of sand-processed clay mixtures with calcium chloride solutions. Journal of Geotechnical and Geoenvironmental Engineering, **124**(3): 231–241. doi:10.1061/(ASCE)1090-0241(1998)124:3(231).

Tinjum, J.M., Benson, C.H., and Blotz, L.R. 1997. Soil-water characteristic curves for compacted clays. Journal of Geotechnical and Geoenvironmental Engineering, **123**(11): 1060–1069. doi:10.1061/(ASCE)1090-0241(1997)123:11(1060).

van Genuchten, M.Th. 1980. A closed-form solution for predicting the hydraulic conductivity of unsaturated soils. Soil Science Society of America Journal, **44**(5): 892–898. doi:10.2136/sssaj1980.03615995004400050002x.

Wang, X., and Benson, C.H. 2004. Leak-free pressure plate extractor for measuring the soil-water characteristic curve. Geotechnical Testing Journal, **27**(2): 1–10. doi:10.1520/GTJ11392.

Xanthakos, P.P. 1979. Slurry walls. McGraw-Hill, New York, N.Y.

Yeo, S.-S., Shackelford, C.D., and Evans, J.C. 2005. Consolidation and hydraulic conductivity of nine model soil–bentonite backfills. Journal of Geotechnical and Geoenvironmental Engineering, **131**(10): 1189–1198. doi:10.1061/(ASCE)1090-0241(2005)131:10(1189).

Yeom, S. 2010. Hydraulic sustainability of soil–bentonite cutoff walls subjected to cyclic wetting and drying. M.Sc. thesis, Department of Civil and Environmental Engineering, Bucknell University, Lewisburg, Pa.